


Development and decline of the ancient harbor of Neapolis

Valentino Di Donato¹ | Maria R. Ruello¹ | Viviana Liuzza¹ | Vittoria Carsana² |
Daniela Giampaola² | Mauro A. Di Vito³ | Christophe Morhange⁴ | Aldo Cinque¹ |
Elda Russo Ermolli¹ 

¹Dipartimento di Scienze della Terra, dell'Ambiente e delle Risorse, Università di Napoli Federico II, Naples, Italy

²Soprintendenza Archeologia Belle Arti e Paesaggio per il Comune di Napoli, Naples, Italy

³Istituto Nazionale di Geofisica e Vulcanologia, sezione Osservatorio Vesuviano, Naples, Italy

⁴CNRS, IRD, Coll France, CEREGE, Université Aix Marseille, Aix-en-Provence, France

Correspondence

Russo Ermolli, Dipartimento di Scienze della Terra, dell'Ambiente e delle Risorse, Università di Napoli Federico II, Naples, Italy.

Email: elda.russoermolli@unina.it

Paola Romano, in memoriam

Scientific editing by Jamie Woodward

Abstract

Archaeological excavations, undertaken since 2004 for the construction of the new Naples subway, have unearthed the harbor basin of the Greco–Roman town of Parthenope–Neapolis, furnishing scientists with the opportunity to recover abundant archaeological remains and a thick succession of diverse infill sediments. The latter underwent sedimentological, paleontological, and volcanological analyses. Compositional data analysis, applied to all three data sets, highlighted three main paleoenvironmental changes in the harbor basin from the Augustan Age up to the 6th century A.D. The beginning of harbor activity is recorded during the 3rd century B.C. when sedimentation was interrupted by intensive dredging of the sea-bottom. The impact of the A.D. 79 Vesuvius eruption, recorded for the first time in the Neapolitan territory, led to a reduction in Posidonia meadows and to an ensuing phase of more restricted water circulation and pollution. At the beginning of the 5th century A.D., an open lagoon environment was established, attesting to coastal progradation. The final closure of this part of the bay occurred at the end of the 5th to the beginning of the 6th century A.D., due to increased alluvial input linked to both natural and anthropogenic causes.

KEYWORDS

A.D. 79 eruption, compositional data analysis, Greco–Roman period, molluscs, geoarchaeology, Naples

1 | INTRODUCTION

During the last 15 years, geoarchaeological investigations associated with the construction of the new Naples subway in Italy have shed new light on the presence and configuration of the Greco–Roman harbor and its surroundings in an excavation area of more than 40,000 m². This study offered the possibility to collect large amounts of stratigraphic and biosedimentological data, which have significantly improved our knowledge about the history of the Greco–Roman town and the evolution of its coastal landscape.

The main phases of ancient harbor activity and the reconstruction of shoreline fluctuations have been debated in numerous publications (Amato et al., 2009; Carsana et al., 2009; Cinque et al., 2011; Giampaola & Carsana, 2010; Giampaola et al., 2006; Ruello, 2008). In particular, the results of geoarchaeological field surveys in the excavation area of Line 1, carried out between 2002 and 2007, confirmed the hypothesis concerning the presence of a Greco–Roman harbor in the modern Municipio Square (Capasso, 1895). Investigation of the ancient harbor stratigraphic sequences allowed us to reconstruct a continuous

history of harbor activity from the 3rd century B.C. to the 5th century A.D. Morphostratigraphy and pollen analysis revealed the natural and cultural landscapes of the harbor catchment from the Greco–Roman up to the Late Roman periods, highlighting the presence of mixed oak woods and tree crops (walnut, chestnut, and grapevines) on the slopes surrounding the town and of vegetable gardens with cabbages around the harbor area (Russo Ermolli, Romano, Ruello, & Barone Lamuga, 2014).

Since 2012, the opening of new excavation areas (Line 6 and Area 4) in Municipio Square provided the opportunity to further improve geoarchaeological knowledge regarding the history of the ancient harbor and its paleoenvironmental evolution between the Hellenistic period and 5th century A.D. This goal has been achieved through a multimethodological approach, including sedimentology, archaeology, macro- and micropaleontology, volcanology, and geostatistics.

The geoarchaeological study of the ancient harbor of Naples is a recent example of a new area of inquiry that considers ancient harbors as exceptional base-level archives in which the sedimentological record and the environment are the result of both geological

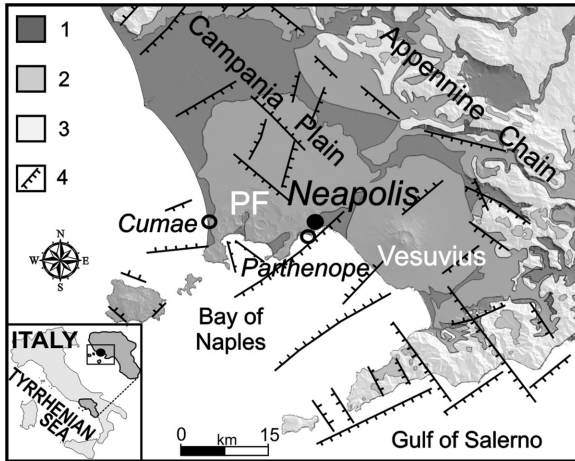


FIGURE 1 Geological and structural setting of the Campanian Plain and location of the archaeological sites cited in the text. PF: Phlegrean fields; 1) Quaternary sedimentary deposits; 2) Quaternary volcanic rocks and sediments; 3) pre-Quaternary units; 4) main faults

processes and human activity (e.g., Marriner & Morhange, 2007; Marriner, Morhange, Flaux, & Carayon, 2017; Morhange et al., 2003, 2015, 2016; Sadori et al., 2015). In the present study, we adopt compositional data analysis methods (CoDA; Aitchison, 1986) to probe the sedimentological and paleontological data. Despite the advanced statistical framework which is now available to analyze compositional data (Pawlowsky-Glahn & Buccianti, 2011), until now relatively few studies have adopted this approach on proxies for paleoecological reconstructions (Di Donato, Martin-Fernandez, Daunis-i-Estadella, & Esposito, 2015; Kaniewski et al., 2013; Rossi et al., 2015; Sgarrella, Di Donato, & Sprovieri, 2012). Sedimentological and paleontological data acquired in the new archeological excavation area of Municipio Square (Liuzza, 2014) provide the opportunity to carry out a paleoenvironmental reconstruction of harbor sedimentation based on an integrated compositional approach.

2 | GEOLOGICAL AND ARCHAEOLOGICAL SETTING

The town of Naples lies in the Campania Plain, a tectonic depression located along the western Tyrrhenian margin of the Southern Apennine chain (Fig. 1), which has been subsiding since the Early Pleistocene (Brancaccio et al., 1991; Cinque et al., 1997; Caiazza et al., 2006). The urban territory currently spreads over a wide area of active volcanism and tectonics, between the eastern edge of the nested caldera of the Phlegraean Fields (PF) and the Vesuvius stratovolcano apron (Fig. 1). During the Late Pleistocene and the Holocene, the Naples area was affected by the deposition of thick tuff deposits and sequences of pyroclastic fallout and density current deposits, mainly erupted by PF and subordinately by the largest Plinian eruptions of Vesuvius.

The geomorphological setting of the study area is the result of a complex interplay among endogenous, exogenous, and anthropogenic

factors. The landscape of Naples is therefore primarily characterized by landforms (such as positive and negative volcanic forms and their remnants) linked to the late Quaternary activity of the PF (last eruption Monte Nuovo, A.D. 1538). In particular, the landscape is the result of the mantling of preexisting volcanic edifices by the 15 ka Neapolitan Yellow Tuff (Deino, Orsi, De Vita, & Piochi, 2004), of the collapse of the related caldera (PF depression) and, between 15 and 3.8 ka, of the accumulation of products from at least 70 explosive eruptions of variable magnitude which generated variably dispersed pyroclastic deposits and formed tuff cones, tuff rings, and lava domes (Di Vito et al., 1999). These morphologies are cut by SW-NE and NE-SW fault scarps, widely spread in the study area (Amato et al., 2009; Cinque et al., 2011; Romano et al., 2013) due to the intense volcano-tectonics (Fig. 1) detected within the PF caldera, the Bay of Naples, and the Campania Plain (Bruno, Rapolla, & Di Fiore, 2003; Cinque et al., 2011; Di Vito et al., 1999). A sequence of depositional and erosional processes, accompanied by fault re-activation, further outline the morphology of this area, together with widespread anthropogenic deposits, reworked by a long-term human activity.

The Naples area was also affected by deposition of two Plinian eruptions of Vesuvius: the Avellino eruption during the Early Bronze Age (Di Vito et al., 2009 and references therein) and the Pomice di Pompei eruption in A.D. 79 (Sigurdsson, Cashdollar, & Sparkes, 1982). These two eruptions were characterized by similar dynamics, with sequences of magmatic phases dominating the main part of the eruptions and minor phreatomagmatic explosions occurring in the last eruption phases (Cioni, Bertagnini, Santacroce, & Andronico, 2008). The magmatic phases are characterized by deposition of widely dispersed pumice fallout sediments distributed in the eastern sectors of the Somma-Vesuvius, whereas the phreatomagmatic phases generated pyroclastic density currents forming thinly laminated-, plane parallel to dune bedded-, or massive-ash beds distributed in the plains surrounding the volcano (Cioni et al., 2008; Di Vito, Castaldo, de Vita, Bishop, & Vecchio, 2013).

The coastal landscape is characterized by hilly terrains with alternating cliff promontories and small bays or narrow coastal plains. These conditions provided natural resources and protected landing places favoring human settlements since prehistoric times (Amato et al., 2009; Carsana et al., 2009; Cinque et al., 2011; Romano et al., 2013). At the end of the 8th to beginning of the 7th century B.C., Greek colonists from Cumae founded at the foot of South Martino Hill and on Megaride Island the settlement of Parthenope (Fig. 2). The necropolis of via Nicotera and ceramics recovered from Chiatamone and the South Maria degli Angeli landfill, dated between the end of the 8th and the 5th centuries B.C., are the only archaeological evidence of this ancient center (Fig. 2).

Farther toward the eastern edge of Parthenope, a new polis, Neapolis, was founded at the end of the 6th to beginning of the 5th century B.C. (D'Agostino & Giampaola, 2005) on the gently sloping area of Pendino (Figs 1 and 2). Parthenope survived as a minor center named Palaepolis (old-polis) until the 4th to 3rd centuries B.C. The Neapolis urban setting is well known and includes the road network (*strigas*), fortifications, necropolis, aqueduct, main public monuments, and villas (AA.VV., 1985; Napoli, 1959, 1967; Stazio, 1988; Zevi, 1995).

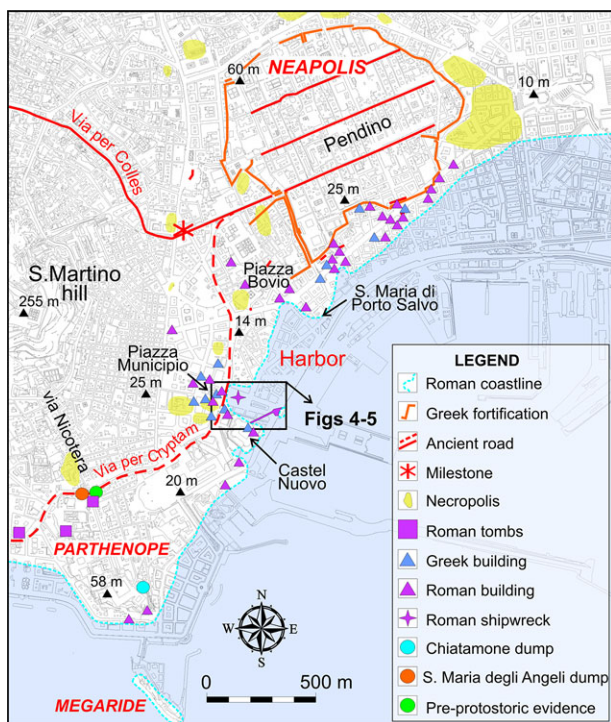


FIGURE 2 Archaeological setting of Parthenope and Neapolis. The box indicates the harbor area as detailed in Figures 4 and 5 [Color figure can be viewed at [wileyonlinelibrary.com](#)]

The excavations for Line 1 of the new Naples subway allowed reconstruction of the ancient coastal landscape, confirming the existence of a wide and sheltered bay between Neapolis and Parthenope (Fig. 2), and demonstrated that the Municipio embayment was the port since at least the 3rd century B.C. when intensive dredging of the sea bottom removed almost all the older sediments (Carsana et al., 2009; Giampaola & Carsana, 2005; Giampaola et al., 2006). The harbor was functional during the Roman Imperial age and up to the beginning of the 5th century A.D. when a lagoon environment became established in the bay. The final closure of this sector of the bay occurred during Late Roman times due to increased sedimentation (Amato et al., 2009; Carsana et al., 2009; Cinque et al., 2011).

3 | NEW GEOARCHAEOLOGICAL DISCOVERIES

New geoarchaeological excavations carried out for Line 6 and Area 4 expanded our previous knowledge about the harbor and ancient coastal landscape. In particular, the ancient harbor extension was more precisely delineated in a suburban position, not far from the Neapolis fortifications. The large inlet hosting the harbor extended from Piazza Bovio to Piazza Municipio, limited to the east by the relief of South Maria di Porto Salvo and to the west by the hill of Castel Nuovo. Archeological surveys and classification of a large number of ceramics (Fig. 3) ensured a very detailed chronology of the investigated sediments, spanning from the 3rd century B.C. to the 6th century A.D. On the whole, this chronology is in agreement with that already defined



FIGURE 3 The sea-floor of the Imperial Age harbor with ceramics dated to the first half of the 1st century A.D. [Color figure can be viewed at [wileyonlinelibrary.com](#)]

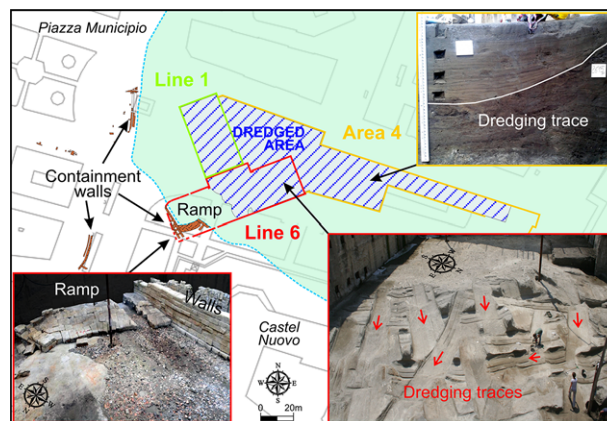


FIGURE 4 Piazza Municipio area and plan of the excavations. The main archaeological findings of 3rd to 2nd century B.C. are indicated together with details of the dredging operations [Color figure can be viewed at [wileyonlinelibrary.com](#)]

in the excavations of Line 1 (Carsana & Del Vecchio 2010; Carsana & Guiducci, 2013; Carsana, D'Amico, & Del Vecchio, 2007; Giampaola et al., 2006). The pottery, often well preserved, represents goods and ship equipment lost during loading and unloading operations in the harbor, or waste from the surrounding suburban areas (Fig. 3). Apart from the chronological value, this large and diversified recovery provides exceptional evidence of the economy and commercial trades of the town.

A few pottery remains coeval with the foundation of Parthenope were found in the dredged marine sediments. This discovery, together with the recovery of sea-bottom deposits saved from the dredging phases, dated to the end of the 6th to beginning of the 5th century B.C., is perhaps evidence for the use of this bay as a harbor during the Archaic period. The existence of the harbor basin is certainly attested by archeological evidence from the 3rd to 2nd centuries B.C. when intensive dredging phases of the sandy-mud infilling were undertaken with the aim of deepening the sea bottom (Fig. 4). The same evidence was already identified in the excavations of Line 1 (Carsana et al., 2009). Important structures discovered in Line 6, such as a probable

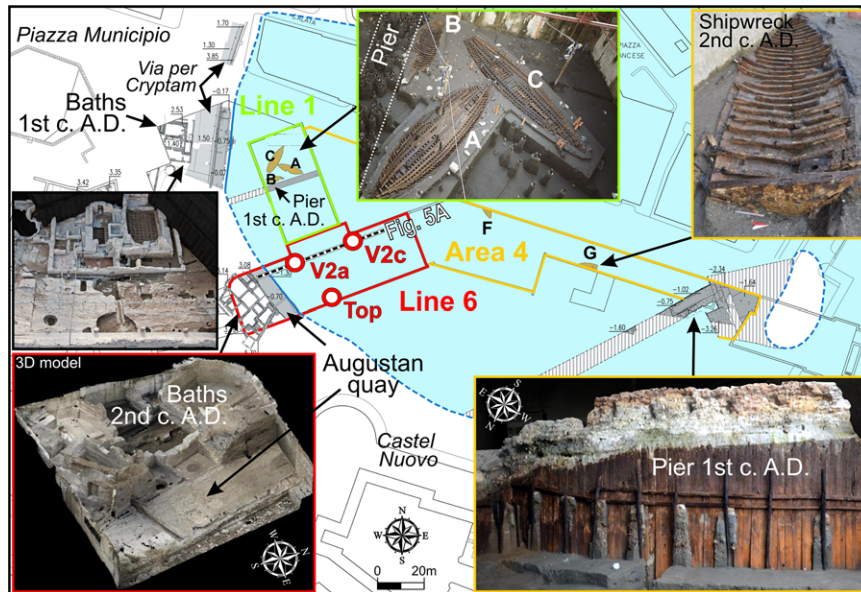


FIGURE 5 The same area as shown in Figure 4 with the main Imperial Age findings. The red circles indicate the position of the investigated sections V2a, V2c and top. The dashed line represents the cross section of Figure 6A [Color figure can be viewed at wileyonlinelibrary.com]

haulage ramp and containment walls for terracing the slope at the rear of the western edge of the harbor (Fig. 4), are dated to the same period. The survey also revealed the sea bottom stratigraphy from the Republican to the late Imperial Age and two poorly preserved shipwrecks dated to the 2nd century B.C. Another two shipwrecks (F and G in Fig. 5), dated to the end of the 2nd century A.D., were unearthed in the central part of the basin. These discoveries expand upon what was already unearthed in Line 1 where two shipwrecks dated to the end of the 1st century A.D. and one of the 2nd century A.D. (B) were found near a wooden pier dated to the end of 1st century A.D. (Carsana et al., 2009; Giampaola & Carsana, 2005; Giampaola et al., 2006).

In addition to the stratigraphy, shipwrecks, and pottery remains, the new excavation unearthed part of the Augustan Age harbor infrastructure and important buildings located along the coastal strip. Along the southeastern edge of the inlet (Area 4), a pier composed of two arms built in cement mortar within a wooden formwork, extends across an area of about 360 m² (Fig. 5). It represented a complex system conceived to create an artificial closing of the port to protect it from the southern winds.

The southwestern part of the protected inlet is equipped with a quay unearthed in two areas, which represented the coastline profile of the ancient harbor until the early 5th century A.D. (Fig. 5). To the rear of the northern quay, a wide road develops, very probably the *via per cryptam* (Fig. 5), commissioned by the Emperor Augustus to connect Neapolis and the PF. At the beginning of the 1st century and continuing into the 2nd century A.D., thermal baths rose along its trace (Fig. 5).

The southern quay, 6.5 m wide and 3.5 m high, extends in a NW-SE direction for 24.5 m. It is built with tuff stones in a cement mortar resting on two rows of squared blocks overlaying the top of tuffaceous bedrock. The latter was reshaped by an artificial cut conceived for lowering the base of the structure in order to create a higher water column close to the quay (Fig. 6A). The depth was ≈ 3 m, based on the relative sea-level (RSL) position at that time, which was ≈ 1.60 m below sea

level (b.s.l.). The RSL was deduced from the upper limit of the marine biomarkers (e.g., serpulids, vermetids, balanids, ostrea, etc...) found in the maximum concavity of the tidal notch, recovered along the quay front (Fig. 6B).

The sediments that accumulated from the base of the Augustan quay up to the beginning of the 6th century A.D. represent the main object of the present work and were analyzed using sedimentological, paleontological, and volcanic proxies. These sediments recorded the history of the harbor bay, revealing both the natural and anthropogenic events that impacted its environment. Ash deposits in the harbor, related to the A.D. 79 eruption, were also investigated. This is the first evidence for the presence of these deposits in the urban Neapolitan territory, mainly due to the lack of stratigraphic information in a densely urbanized context. The stratigraphic continuity of the studied sequences is only interrupted, in a very limited area immediately close to the quay, by a new dredging phase after the A.D. 79 eruption. This action, recognized through a series of parallel trenches (Fig. 6C), aimed at maintaining a functional water depth suitable for docking, after the increased sediment supply due to the eruption.

4 | SEDIMENTOLOGICAL AND PALEOECOLOGICAL ANALYSES OF THE HARBOR SEDIMENTS

Sediments of Neapolis harbor dating from the Augustan Age up to the beginning of the 6th century A.D. were investigated by means of an integrated approach including granulometric, volcanological, micro- and macropaleontological analyses. CoDA methods were applied to both granulometric and macrofaunal data, involving relative variation biplots (RVB; Aitchison & Greenacre, 2002), simplicial principal components analysis (SPCA; Aitchison, 1983), and cluster analysis based on Aitchison distances. Ostracod data were too scanty and incomplete

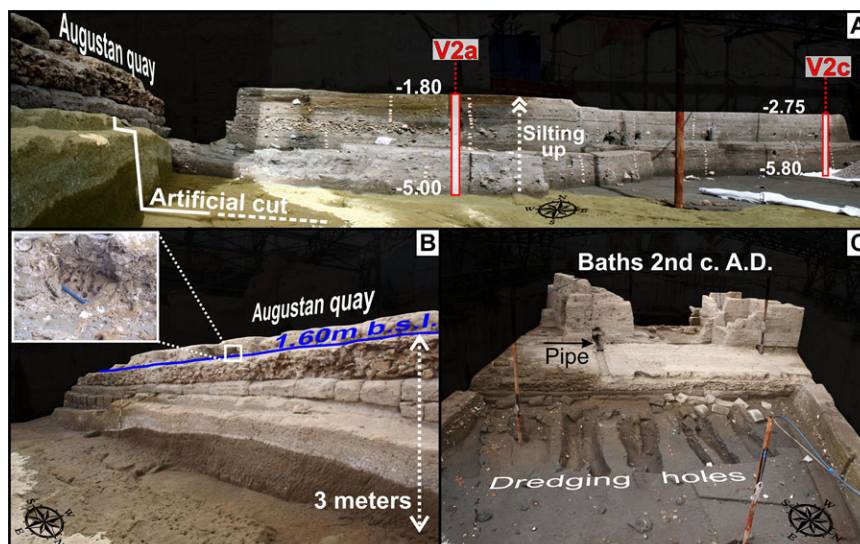


FIGURE 6 A) On the left side, the Augustan quay and artificial cut into tufaceous bedrock; in the background, the investigated infill sediments with position of the studied sections; B) frontal view of the Augustan quay with sea level position and water column as inferred from marine biomarkers; and C) general view of the Augustan quay and of the thermal baths with evidence of the drainage pipe. Dredging holes placed in front of the quay after deposition of the A.D. 79 eruptive event [Color figure can be viewed at wileyonlinelibrary.com]

for this kind of approach. The paleoecological interpretation of fossil assemblages was based on the modern ecological requirements of the identified mollusk taxa, as summarized in Supplemental Table 1. All methods are detailed in the Supplemental Text.

4.1 | The analyzed sections

The analyses were carried out on two stratigraphic sections, V2a and V2c, located 11 m and 35 m from the Augustan quay, respectively (Fig. 5). Section V2a is 3.20 m thick, extending 1.80–5.00 m b.s.l. (Fig. 6A). The beginning of sedimentation in this bay sector, exposed in section V2a, directly lies above the artificial cut in the tufaceous bedrock, related to the quay construction. Twenty-five samples were collected along this section, each sample corresponding to a different archeostratigraphic unit (AU). Section V2c is 3.05 m thick, extending 2.75–5.80 m b.s.l. (Fig. 6A). In this bay sector, the sediments analyzed in section V2c lie above the last surface (2nd century B.C.) of the dredged sea-bottom sands (Fig. 4). Moreover, the V2a–V2c transect is not affected by the 1st century A.D. dredging, which was limited to areas near the quay (Fig. 6C). Eighteen samples were collected along this section and, as for section V2a, each sample corresponds to a different AU. The sections cover a time interval spanning from the 1st century B.C. to the 6th century A.D. The uppermost interval of deposition, corresponding to the end of the 5th–beginning of 6th century A.D., was removed before sampling in both sections for technical reasons linked to the construction of engineering structures for the subway station. Thus, samples covering this uppermost interval were obtained from a different vertical profile (“Top” section in Fig. 7), in the southern sector of the excavation site. In both sections, a 50 cm thick volcaniclastic level was observed, with lenses of subrounded, centimetric to subcentimetric pumice lapilli, whose sedimentology and lithology suggest that they are reworked deposits of the A.D. 79 Pompeii erup-

tion (see below). As in the sediments of Line 1, *Posidonia oceanica* remains (Cennamo, Caputo, Stefano, Russo Ermolli, & Barone Lumaga, 2014) are abundant throughout the sequence.

4.2 | Granulometric analysis

Granulometric data are summarized into a ternary diagram (Folk, 1954) in which gravels, sands, and muds (silt and clay) are considered as parts of the composition (Fig. 8A). In both sections, coarser samples are those dated to the second half of the 1st to the 3rd centuries A.D. and from the first half of the 5th to the beginning of the 6th century A.D. All samples show a low degree of sorting (Fig. 7), indicating that the marine processes did not have the competence to rework the sediment that is often deposited rapidly and continuously at base level. Since sand is the major component of most samples, the variability of samples can be better highlighted in a centered ternary diagram in which both samples and grids are centered with respect to the compositional center of the data (Eynatten, Pawlowsky-Glahn, & Egozcue, 2002; Fig. 8B). On the basis of cluster analysis (see Supplementary Text for details), four groups of samples were distinguished (Fig. 9A).

In order to define the characteristics of the clusters, an SPCA of granulometric data was undertaken (Fig. 9). The isometric-log-ratio (ilr) (Egozcue et al., 2003) principal component 1, which accounts for most of the samples’ variability (about 83%), is almost parallel to ilr2 axis, indicating that the main source of variability is related to relative changes between gravel and mud (Fig. 10A). A secondary source is related to relative changes of sand with respect to the other components. This result is also evident in the ternary diagram, showing the back-transformed principal components axes (Fig. 10B). The cloud of samples is elongated in a direction forming a high angle with balance 1 axis. As shown by the confidence ellipses of Fig. 10A, samples belonging to the sections V2a and V2c appear distinguished in the ilr space.

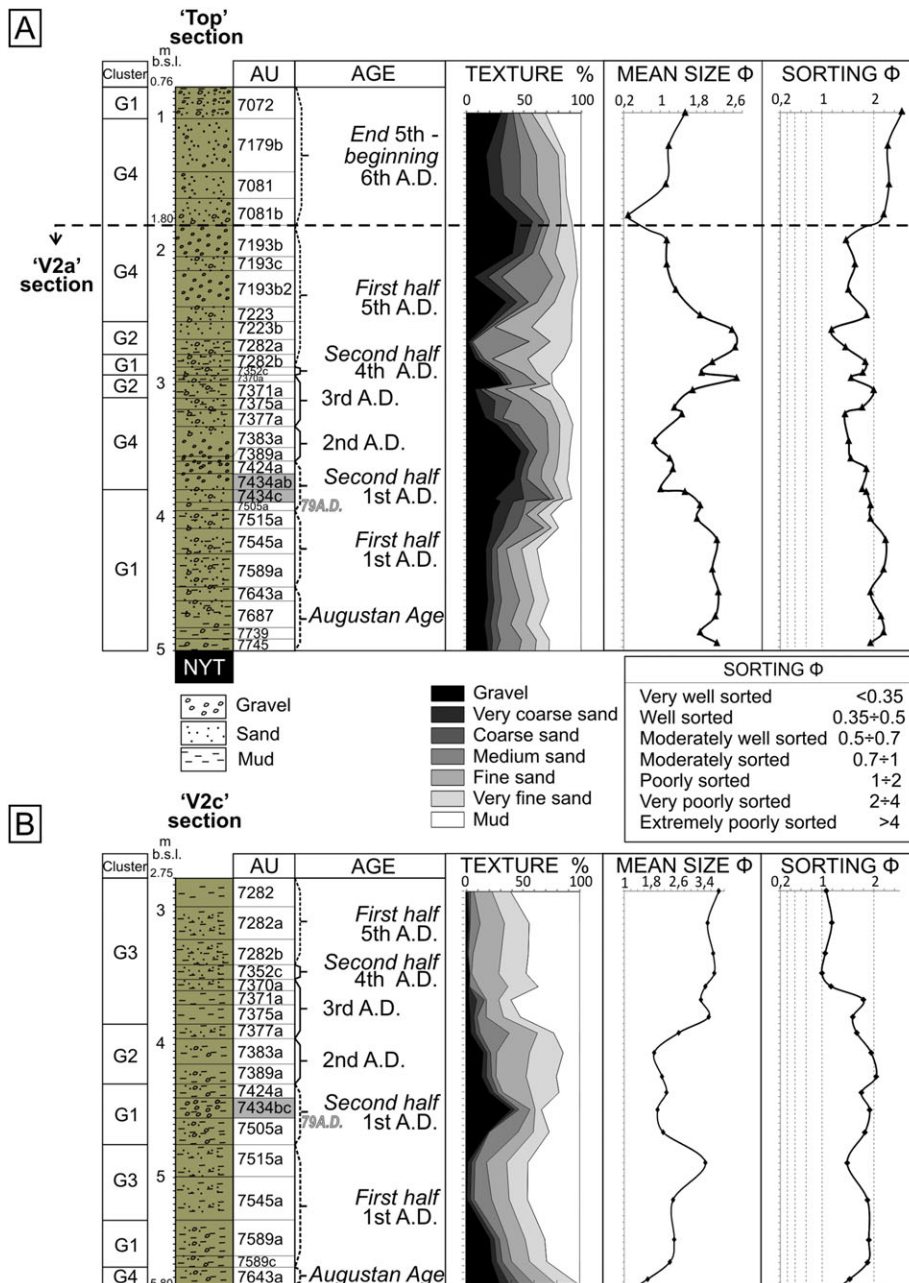


FIGURE 7 Granulometric data and Folk statistical parameters for log V2a (A), top section (A) and log V2c (B). Most samples show a low degree of sorting, ranging between 1 and 2 ϕ [Color figure can be viewed at wileyonlinelibrary.com]

Indeed, a multivariate analysis of variance (MANOVA) performed on ilr coordinates indicates that these two groups of samples are significantly different at an alpha level of 0.05.

Clusters G4 and G3 are characterized by high and low gravel to mud log-ratios, respectively. Clusters G1 and G2 are located closer to the origin of axes and are distinguished by the relative abundance of sand, which is higher in cluster G2 (Fig. 10B).

4.3 | Paleontological analysis

Ostracods show a general dominance of coastal assemblages (mainly *Loxocochna romboidea*, *Aurilia convexa*, *Leptocythere rara* and *Ponthocythere elongata*) all along the lower interval of both sections (Fig. 11).

Towards the upper part of both sections, this assemblage shows a decreasing trend and is replaced by the lagoon species *Xestoleberis* sp. (Fig. 11). The uppermost levels, only present in section V2a, are devoid of ostracods. The general paucity of ostracods (i.e., 10 specimens in 100 g) and their fragmentation did not allow the application of the CoDA approach to these data.

Mollusk assemblages found in logs V2a and V2c are shown in Fig. 11. *Bittium reticulatum* is a fundamental component of the assemblages, notwithstanding a decreasing trend, more marked in log V2a. In general, apart from the uppermost intervals, a large part of the assemblages is constituted by taxa related to bottom vegetation, mainly represented by *Posidonia oceanica* meadow, as testified by its remains commonly found in the sediments. *Paphia aurea* and *Loripes lucinalis* are rare

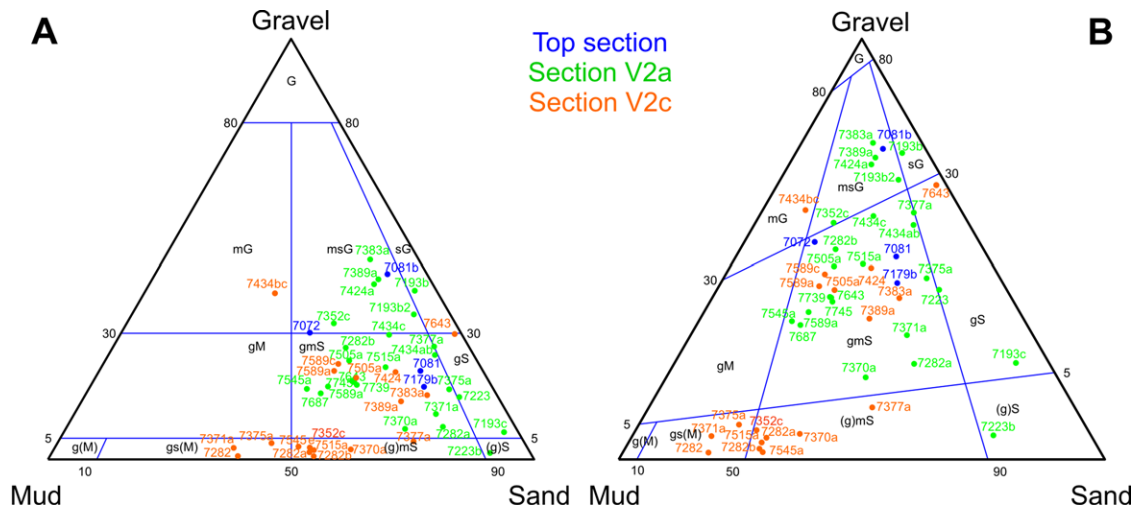


FIGURE 8 A) Granulometrical data reported as a gravel, sand, and mud ternary diagram (Folk, 1954). Orange dots (black in printed version): log V2c; green dots (dark grey in printed version): log V2a; blue dots (light grey in printed version): top section. Labels refer to the archaeostratigraphical units. B) The same data of diagram A, centered by perturbing the composition with the inverse of the compositional center of the dataset (see "Supplementary text"). Note that both sample points and grids are centered [Color figure can be viewed at wileyonlinelibrary.com]

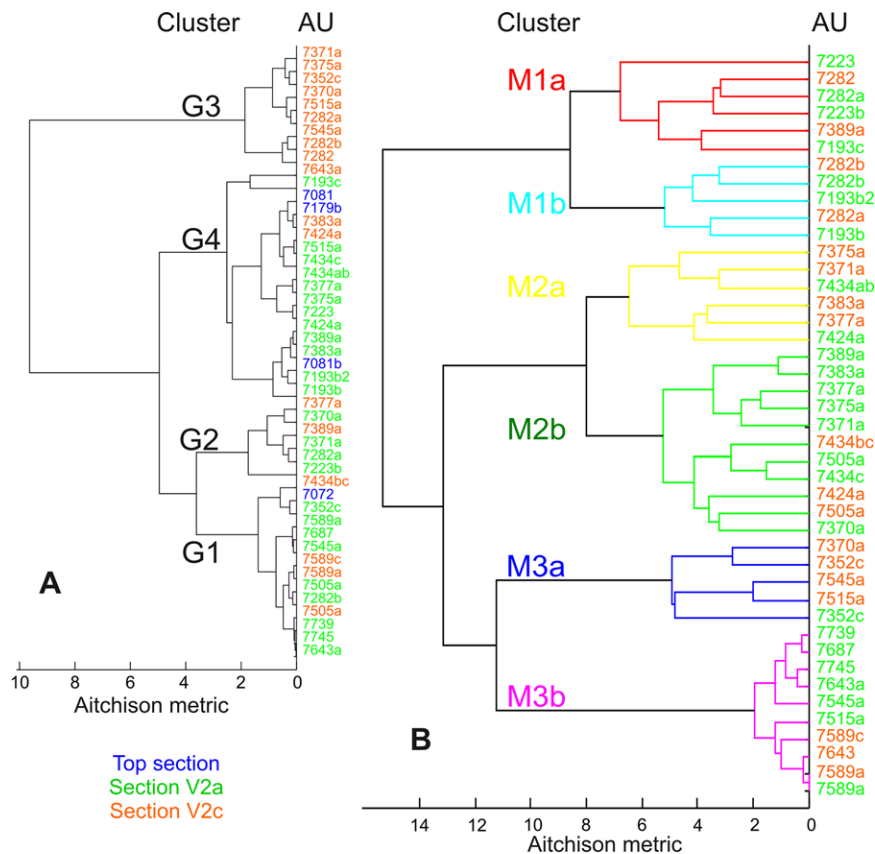


FIGURE 9 A) Cluster analysis of granulometric data (Ward's method based on Aitchison distances, i.e., the Euclidean distances on \ln coordinates). The number of clusters is defined by means of Mojena index. B) Cluster analysis of mollusk assemblages [Color figure can be viewed at wileyonlinelibrary.com]

or missing in the lower interval of both sections. *Cerastoderma glaucum*, which is also rare in the lower intervals, increases in the uppermost part of both sections.

As with the granulometric data, mollusk assemblages were analyzed by means of cluster analysis (Fig. 9B). In order to better highlight

the relationship among taxa and between taxa and samples, the three obtained clusters, each of them further divided in two subclusters, were considered to distinguish row points into the RVB (Fig. 12).

The first three axes of the RVB account for about 70% of the total variability. The relationships observed along the first axis of the biplots

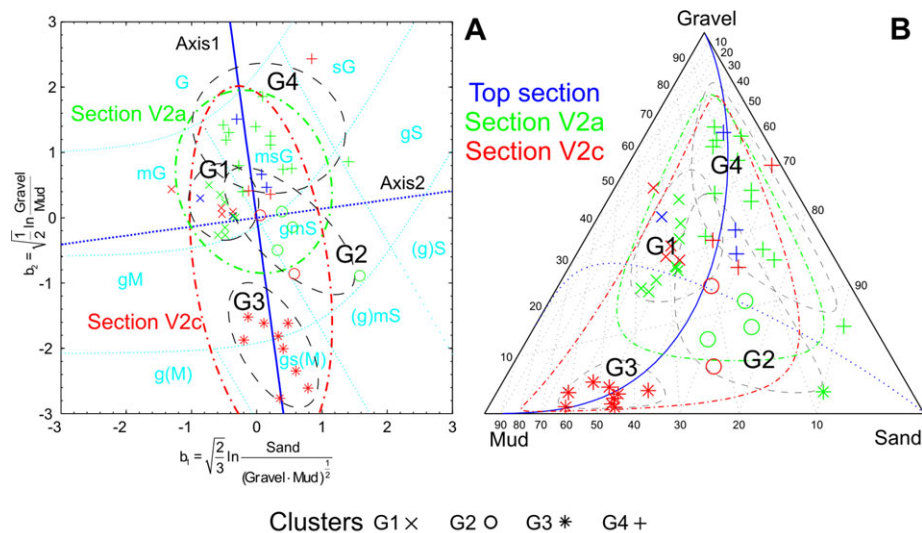


FIGURE 10 A) Scatter plot of balances 1 and 2. Balance 1 expresses the log contrast between sand and other components, balance 2 the log contrast between gravel and mud (see “Supplementary text”). The continuous and dotted dark blue lines (black in printed version) are the principal components of ilr coordinates. The thin dotted lines (light blue; black in printed version) show the fields of the Folk diagram as they appear in ilr space. Colors and symbols of row points indicate the section and the clusters to which they belong; green (dark grey in printed version) samples: log V2a; orange (black in printed version) samples: log V2c.; blue (light grey in printed version) samples: top section. Section samples and clusters are contoured by 2σ confidence ellipses. Dash-dot lines: sections; dashed lines: clusters. B) Simplicial principal components analysis of granulometrical data. Data are centered as in Fig. 8B. Directions of maximum variability in the ternary diagram (dark blue; black in printed version) are obtained by back transforming the principal components of ilr data shown in Fig. 10A. The first direction is related to changes of sand with respect to the other two components, the second to relative changes of gravel versus mud. Dashed and dash-dotted lines show compositional confidence ellipses (coherent with the Aitchison geometry) corresponding to those shown in Fig. 10A [Color figure can be viewed at wileyonlinelibrary.com]

highlight a high variability in the log-ratios between *Bittium reticulatum* or *Nassarius corniculatus*, located at the negative side, and *Cerastoderma glaucum*, *Cyclope neritea* and *Tapes decussatus*, located at the positive side. The column point of *Gibbula* spp., which appears located near the origin of the biplot in a two-dimensional representation, shows an orientation toward the positive side of axis 3 when a third axis is included in the RVB. As a consequence, the links connecting its column point to other taxa form high angles with the links connecting taxa without a significant projection on axis 3 and in particular with those located near the origin of the biplot, such as *Nassarius mutabilis* and the group UCSA. Since the angle between the links connecting column points approximates the correlation between the corresponding log-ratios, this behavior indicates that the relative variation of *Gibbula* spp. with respect to the other taxa tends to be independent from their relative variations.

Additional information was added by including balances 1 and 2, adopted in the sedimentological analysis, as supplementary vectors in the RVB of the mollusk assemblages. The vector of balance 2 is opposed to the *Gibbula* spp. column vector. This indicates that relative increases of this taxon tend to correspond to increases in the mud to gravel ratios. In effect, samples of cluster G3 (having low gravel to mud log-ratios) are mostly located near the *Gibbula* spp. column point, in opposition to the vector of balance 2. The vector of balance 1, which is related to increases in sand versus other components, seems related to high relative abundances of *Cerastoderma glaucum* or *Cyclope neritea* and low relative abundances of *Bittium reticulatum*. Unlike the granulometric data, the mollusk assemblages belonging to the sections V2a and V2c are not well differentiated in the biplot. In effect, the results

of a MANOVA based on the first 3 axis scores (Quinn & Keough, 2002) of the form biplot indicate that sample mean differences are not significant at an alpha level of 0.05.

5 | EVOLUTION OF THE ENVIRONMENTS IN THE HARBOR BAY

The results of sedimentological and paleontological analyses, constrained by chronology, allowed three main paleoenvironmental units to be distinguished along the studied sections from the Augustan Age up to the Late Roman period: marine, transitional, and terrestrial (Fig. 13). This succession of environments reflects the natural evolution of a limited accommodation space, which is gradually filled with sediments (Marriner & Morhange, 2006). In general, the paleoenvironmental changes reconstructed in the two stratigraphic profiles are well correlated and show that the transition from the marine to the lagoon environment occurred at the beginning of the 5th century A.D. The transition from the lagoon to the continental environment occurred at the end of the 5th to beginning of the 6th century A.D., through a short phase of alluvial input into a shallow lagoon environment.

5.1 | The marine environment

5.1.1 | From the Augustan Age up to A.D. 79

In both sections, samples dated to the Augustan Age up to the first half of the 1st century A.D. belong to clusters M3b (Figs 11 and 13).

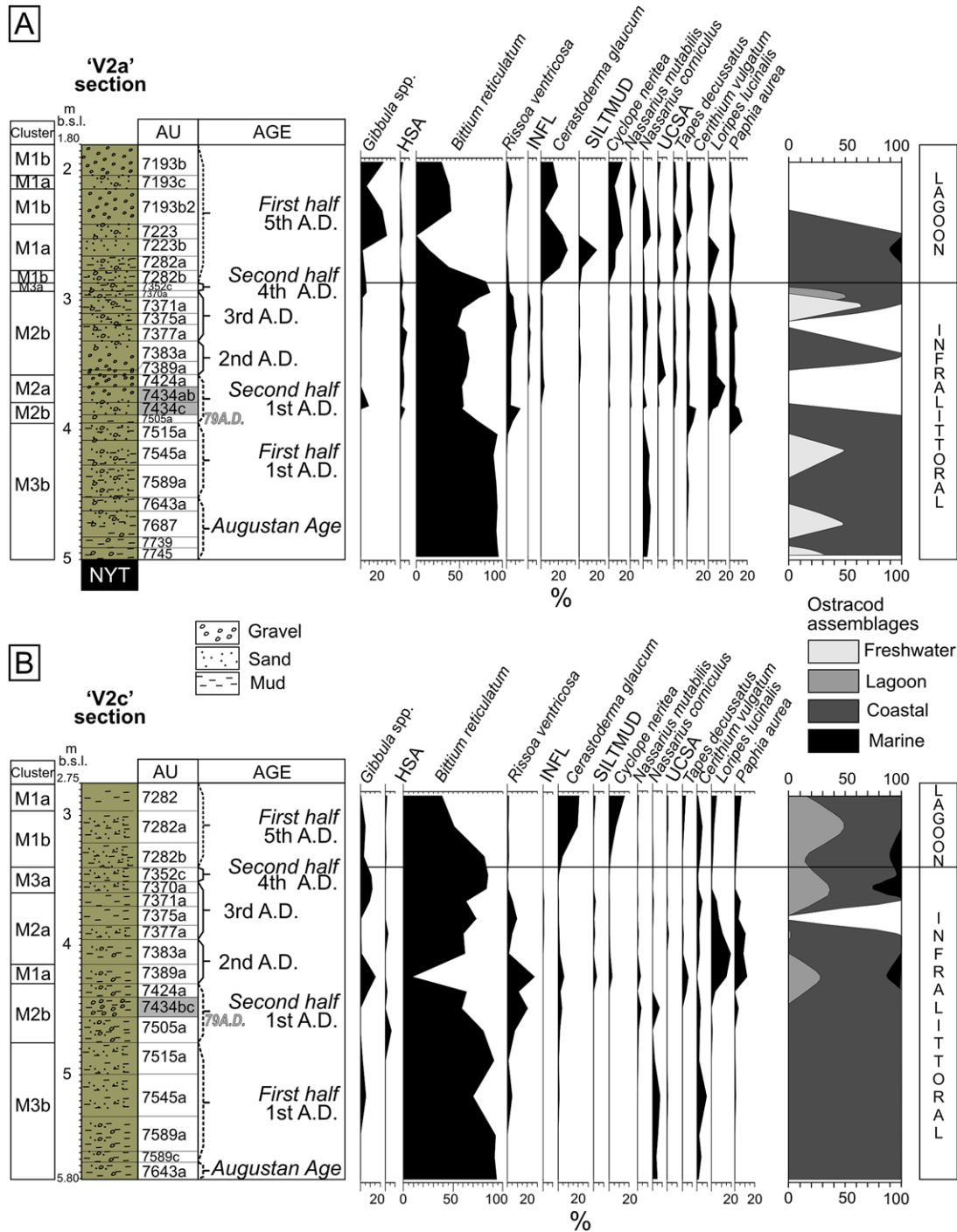


FIGURE 11 Percentage distribution of selected mollusk taxa and ecological groups of ostracods in log V2a (A) and log V2c (B) [Color figure can be viewed at wileyonlinelibrary.com]

As indicated by the location on the negative side of axis 1 of the RVB (Fig. 12), they are characterized by high relative abundance of *Bittium reticulatum* and *Nassarius corniculatus*. Coherently with the abundant remains of *Posidonia oceanica* (Fig. 13), the mollusk and ostracod assemblages (mainly *Aurila convexa*) indicate that a well-developed meadow was present at the sea-bottom from the Augustan Age up to the *Pompeii* eruption. Samples of cluster M3b mostly belong to granulometric cluster G1 (Fig. 12), characterized by low log-ratios between mud and gravel. The results indicate that, during this time interval, the

investigated area of the harbor was characterized by a vegetated (*Posidonia* meadows) low-energy shoreface environment, with a muddy-sandy bottom.

From the first half of the 1st century A.D., the growth of mollusk species associated with a shallower *Posidonia oceanica* meadow is indicated by the relative increase in *Gibbula* spp. in the samples of section V2c assigned to cluster M3b (Fig. 11B). In particular, a general tendency toward a closing of the environment seems to be evident by a change in the malacofauna (Fig. 11). As shown by the position of the row points

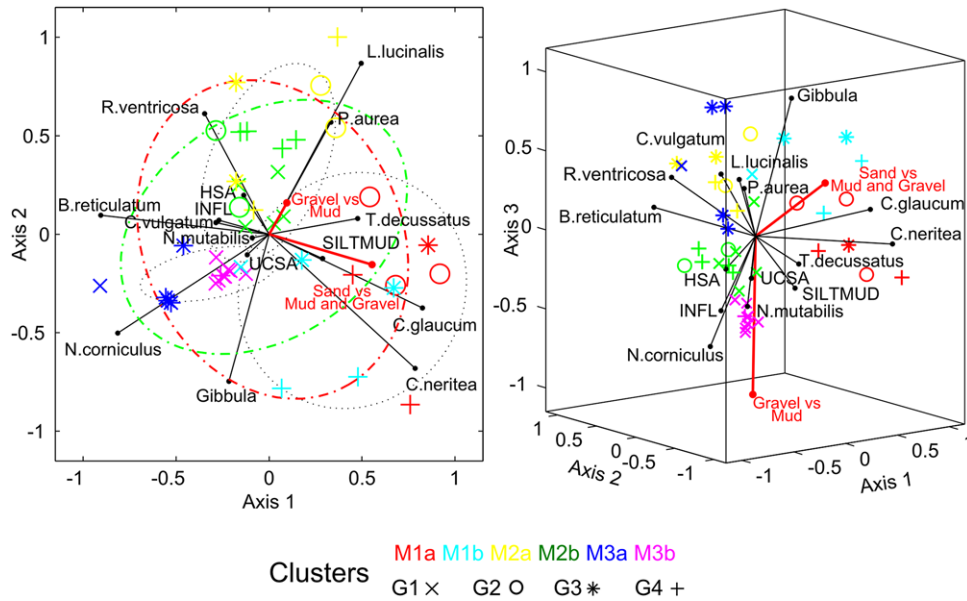


FIGURE 12 Relative variation biplot of mollusk assemblages, showing the first 2 axis (A) and the first three axis (B) obtained from singular values decomposition of clr data (see “Supplementary text”). Sample points are shown with symbols and colors (scaled grey in printed version) to show both the granulometrical and mollusk subcluster to which they belong (see Fig. 9). 2σ confidence ellipses are drawn to contour sections (dashed-dotted lines) and clusters (dotted lines). Bold red (black in printed version) vectors represent the balances obtained from CoDa of granulometrical data: [Color figure can be viewed at wileyonlinelibrary.com]

belonging to cluster M2b (Fig. 12), the second half of the 1st century A.D. (prior to A.D. 79) is marked in both sections by a compositional switch (from M3b to M2b, Fig. 13). In particular, a decrease in the relative abundance of *Bittium reticulatum* and an increase in the relative abundance of opportunistic species, such as *Rissoa ventricosa*, *Paphia aurea* and *Loripes lucinalis* (Fig. 11) is recorded. At the present stage of investigation, it cannot be ascertained if this slight shallowing tendency was determined by natural phenomena, such as the accretion of infratidal bottom sediment, or if it was in some way related to the construction of artificial barriers within the harbor (piers of 1st century A.D.), as pointed out in the Roman harbor of Fréjus in France (Bony, Morhange, Bruneton, & Gébara, 2011).

The apparent rate of sedimentation (ARS) recorded before the A.D. 79 (Fig. 13) shows rather high values, up to 2.5 cm/yr, which can be easily considered as a consequence of the dredging and of the construction of the Augustan quay. In fact, the building of this structure implied the regularization of both the coastline and the sea-bottom through the artificial cut of the tuffaceous bedrock (Fig. 6A), in order to create a water column suitable for shipping. This cut created a new and wide accommodation space that was rapidly filled by sediments. Once the artificial space was filled, the mean ARS lowered to 0.45 cm/yr (mean value) until the A.D. 79 eruption (Fig. 13). This ARS value seems to be the usual rate in this bay, when no disturbing event (anthropic and/or natural) takes place. The intense commercial activity in the harbor during this period, testified by the construction of the quay and the large amount of pottery lost underwater, seems not to have been disturbed by the rapid accumulation of sediments (from ≈ 4.60 to ≈ 3.20 m b.s.l. close to the quay). Considering that the attested sea level was at 1.60 m b.s.l., the water column of ≈ 3.5 to ≈ 2.0 m was still suitable for loading/unloading operations (Boetto, 2010; Poveda, 2012).

5.1.2 | The A.D. 79 eruption and its impact on the marine environment

The A.D. 79 Pompeii eruption generated widespread pyroclastic deposits with widespread impacts around the Somma-Vesuvius (Sigurdsson, Carey, Cornell, & Pescatore, 1985). In particular, the main phase of the eruption was Plinian and dominated by magmatic explosions which generated thick fallout deposits distributed south-eastward of the volcano, including the Pompeii area, the eastern area of the Gulf of Napoli and the Sorrento Peninsula. These deposits are mainly composed of well sorted, white to gray pumice lapilli (Carey & Sigurdsson, 1987). The second main phase of the eruption was dominated by phreatomagmatic explosions which produced pyroclastic density currents radially distributed around the volcano up to a distance of 15 km. The currents emplaced cohesive, cross-laminated to massive, fine-grained ash beds. Archeological excavations (unpublished data by the authors) in the urban area of Naples have revealed that the pyroclastic density current deposits were distributed in many lowlands between the western apron of Vesuvius and the Parthenope area (Fig. 1). This distribution is in agreement with the reconstruction described by Gurioli et al. (2010), abruptly truncated in the urban territory of Naples for absence of data. These deposits have also been recognized in the Municipio area where they are represented by two cohesive and massive ash layers containing accretionary lapilli, thickening in the preexisting lowlands and depressions. The SEM analyses revealed that the majority of the juvenile fragments of the fine ash deposits (Fig. 14) show characteristics such as poorly- to nonvesicular blocky morphologies, alteration skins, pitting and minor quench cracks, and adhering particles, that suggest a predominantly phreatomagmatic origin. This ash deposit is barren. These characteristics corroborate the correlation of these deposits with those of

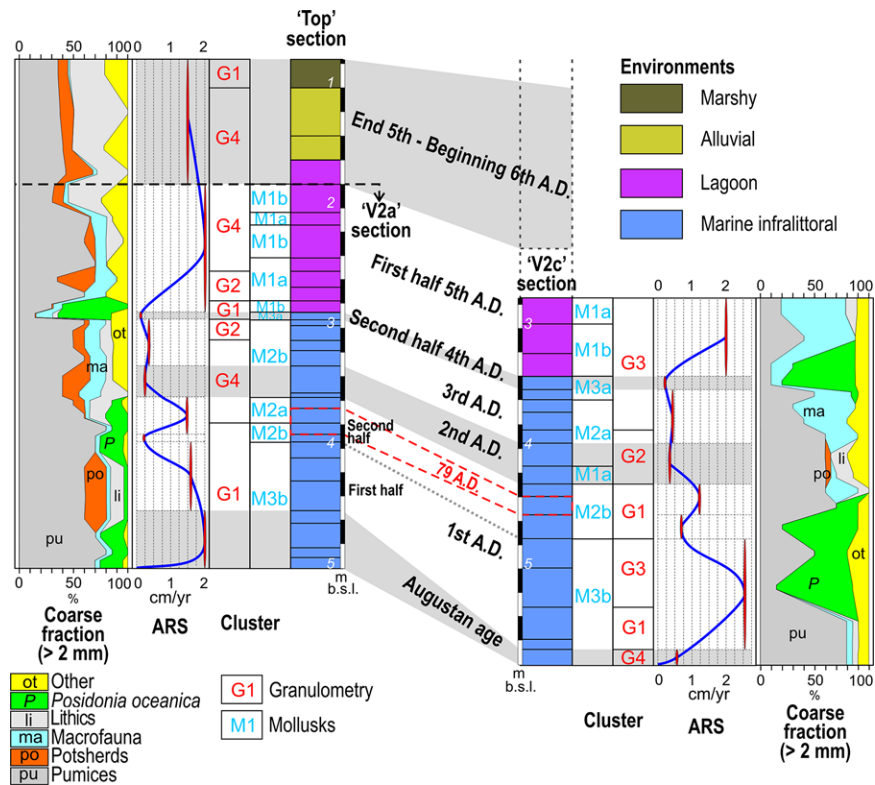


FIGURE 13 Chronostratigraphic sequence of paleoenvironments along the two studied sections compared to the apparent rate of sedimentation (ARS) and to the composition of the coarse fraction (> 2 mm). ARS was calculated by taking into account, for each century, the years represented in the sediments and the corresponding thickness [Color figure can be viewed at wileyonlinelibrary.com]

the phreatomagmatic final phases of the eruption which emplaced pyroclastic density currents, likely flowing inland. Furthermore, the presence of soft accretionary lapilli suggests the absence of reworking of the ash after its deposition. The ash layer is overlain in the two studied sequences by a deposit composed of an alternation of lenses of subrounded to rounded, well sorted pumice lapilli and ash, for a total thickness of about 40 cm (Fig. 15A). The high degree of roundness of lapilli and the structure of this deposit suggest that the pumice lapilli, erupted during the Plinian phase of the eruption (before the phreatomagmatic phase) and distributed southeast of Vesuvius, were transported by marine currents and deposited on the beach after a long phase of reworking. These reworked deposits were interpreted by Delile, Goiran, Blichert-Toft, Arnaud-Godet, and Romano (2016a) as being of a tsunami origin.

On land, the A.D. 79 eruption is only represented by the fine-grained ash deposit (Fig. 15B). The absence of the reworked pumice rich deposits and/or of marine remains, even at short distances and low elevation from the Roman coastline in the whole excavation area, allows us to exclude the speculation of the tsunami driven deposition suggested by Delile et al. (2016a). The hypothesis is also excluded by the absence of damage to buildings and structures in the coastal area.

After A.D. 79, the textural features of the studied sections show increasing variability. As evidenced by the compositional analysis of granulometric data, the main source of variation in V2a section is related to changes in the gravel versus mud ratio, from G1 to G4

(Fig. 13). The changes in the gravel fraction are mainly driven by potsherd inputs from inland and by pumice arrivals (Fig. 13) from both inland and wind-sea currents accumulated near the quay, especially in concurrence with the A.D. 79 eruption deposits and their long-term reworking. The primary deposition coupled with the arrival of reworked volcanic material, caused the increase in the ARS, which reaches values around 1.35 cm/yr (mean value) until the end of the 1st century A.D. (Fig. 13).

Just after A.D. 79 and up to the end of the 3rd century A.D., the *Posidonia oceanica* meadow appears poorly developed (Fig. 13), indicating the occurrence of unfavorable ecologic conditions at the basin bottom. The ostracods, totally absent in V2a between A.D. 79 and the first half of the 2nd century A.D., are still dominated by coastal assemblages and record a significant amount of *Xestoleberis* spp., a lagoon taxon (e.g., section V2c, Fig. 11B). In the same interval, a further decrease in *Bittium reticulatum* and peaks of *Rissoa ventricosa* and *Paphia aurea* are recorded (Fig. 11). In general, the mollusk assemblages belonging to clusters M2a and M2b are indicative of reduced oxygenation, which may also be related to an increase in trophic level and/or pollution within the harbor. Bottom vegetation may be damaged by thick deposits of floating tephra and/or by the subsequent erosion of volcanic material from the catchment, which could enhance water turbidity (Ayris & Delmelle, 2012). If the impact of the A.D. 79 eruption, even if greatly diluted by distance, has caused a temporary change in the sea-water chemistry and turbidity, or even directly induced damage to the bottom vegetation in the harbor of Neapolis, this effect should have been flanked

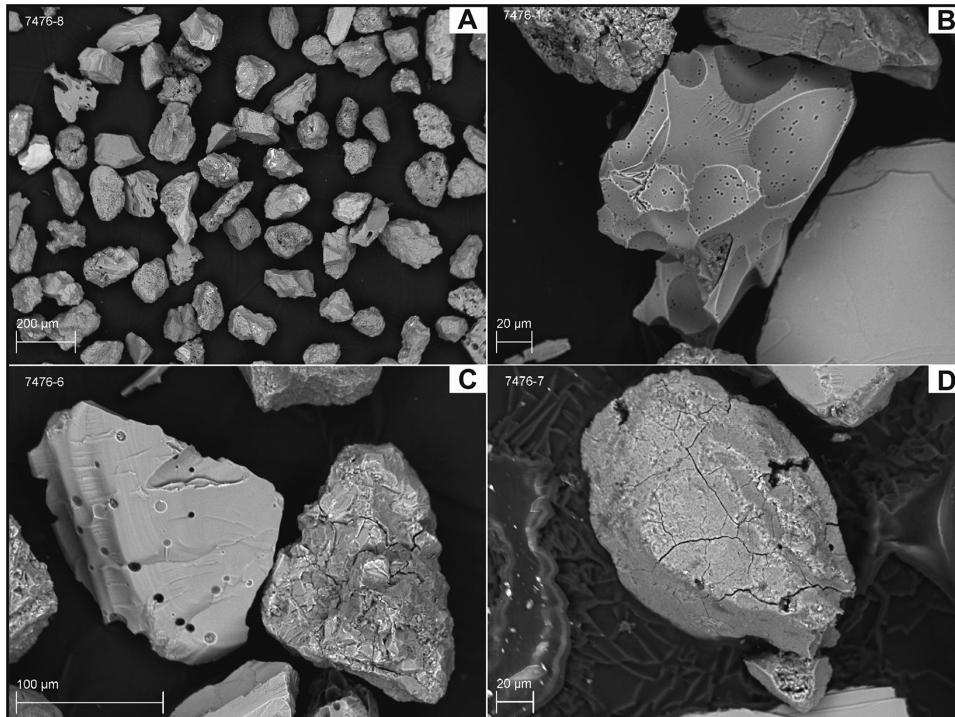


FIGURE 14 SEM images of selected pyroclasts of A.D. 79 ash deposits (AU 7476, Fig. 15B). A) whole sample dominated by nonvesicular clasts; B) weakly vesicular to nonvesicular clasts with pitted surface; C) and D) blocky clasts with adhering particles, alteration skin and quench cracks. All features are typical of fragments generated by phreatomagmatic fragmentation (Heiken, G.H., 1974; Heiken, G. & Wohletz, K., 1985)

and prolonged by other causes. Probably, the concomitant protective effect of piers, increasing sedimentation, and polluting effects of thermal bath drainpipes could have enhanced environment deterioration. Similarly, the construction of harbor facilities both in Marseille (France) and Elaia (Turkey) led to destruction of the original *Posidonia* ecosystem (Morhange et al., 2003; Seeliger et al., 2013).

5.1.3 | From the 2nd to the 4th century A.D

The first tendency toward the establishment of a closed environment, highlighted in the previous period, is enhanced from the first half of the 2nd century A.D., as testified by mollusk assemblages of the outer V2c section, included in cluster M1a, and by the presence of lagoon ostracods (Fig. 11) up to the end of the 4th century A.D. The increase in the high trophic level recorded in the bay until the end of the 3rd century A.D., begins in concurrence with the construction of the Roman baths at the end of the 2nd century A.D. (Figs 5 and 6C), whose drainage pipe flowed into the harbor probably inducing pollution, such as lead enrichment highlighted by Delile et al. (2016b). During this time interval, more or less similar assemblages (M2a and M2b) are found in both sections (Fig. 13). Differently, the results of CoDA show that samples of section V2a are included in the granulometric clusters G4-G2, characterized by a relative abundance of sand and gravel (mainly composed of pumices and potsherd), while those of section V2c fall into clusters G2-G3, characterized by a reduced coarse component and finer sediments. In effect, both sections equally record the pumice and ash arrivals, whereas only in the internal section (V2a), closer to the quay, the anthropic inputs (mostly potsherds and building

stones from harbor structures) are an important component of the coarse sediment fraction during the 2nd century A.D. (Fig. 13) when thermal baths were constructed behind the quay.

Once the large sedimentary input linked to the A.D. 79 eruption and its reworking was expended and the beach profile was regulated, the ARS gradually came back to its usual values (mean value 0.35 cm/yr in the 2nd and 3rd centuries A.D., Fig. 13), similar to those recorded before the eruption. At the beginning of the 4th century A.D., open conditions re-established with the recovery of the bottom vegetation as testified by the increase in *Posidonia oceanica* remains and the occurrence of mollusk assemblages belonging to cluster M3a. The 4th century A.D. is characterized by very low ARS, with mean values ranging around 0.17 cm/yr, which in the internal section may be partly related to the relative decrease in the coarse fraction supplied by the anthropic wastes (Fig. 13). At that time, the quay was no more in use due to the decreasing water column (maximum 1.20 m close to the quay). A stagnation of port activities was recorded in the 3rd–4th centuries A.D. (Giampaola et al., 2006) both in Line 6 and Line 1, where it occurred in concomitance with a phase of abandonment highlighted by the decrease of horticultural activities around the harbor and the development of wild vegetation (Russo Ermolli et al., 2014). Both the lower ARS and the reduced use of the harbor could have favored the environment recovery.

By comparison, Delile et al. (2016a) evaluated a drastic decrease in the rate of sedimentation between the 3rd and the beginning of the 5th century A.D., as well as the absence of the 4th century A.D. levels in their sampling. In order to explain these anomalies, they hypothesize numerous dredging operations carried out in the 3rd and in the



FIGURE 15 A) Evidence of the A.D. 79 eruptive event in the marine environment: the ash layer directly deposited by pyroclastic density currents is overlain by reworked ash, pumice, lapilli, and *Posidonia* remains; B) the A.D. 79 ash primary deposit on land [Color figure can be viewed at wileyonlinelibrary.com]

5th century A.D. However, during the archeological excavations carried out in both Lines 1 and 6 areas for more than 15 years, no chronological gap was recorded in the 4th century A.D. and no evidence of dredging was identified between the 3rd and the 5th century A.D.

5.2 | The Lagoon environment and final harbor closure (beginning of the 5th to beginning of the 6th century A.D.)

The beginning of the 5th century A.D. marks an important paleoecological swing, which was already highlighted in the excavations for Line 1 (Amato et al., 2009; Carsana et al., 2009; Russo Ermolli et al., 2014). The progressive closure of the harbor basin and the consequent transition toward a muddy-sand lagoon context is recorded by an increase in the percentage of lagoon ostracods in section V2c (Fig. 11) and by a change in the composition of mollusk assemblages, which in the upper interval of both sections belong to clusters M1a and M1b (Figs 11 and 13). In the RVB (Fig. 12), samples belonging to cluster M1a are located close to the column points of *Cerastoderma glaucum* and *Cyclope neritea*, indicating high relative abundances of these taxa, which corresponds a decreasing relative abundance of *Bittium reticulatum*. These assemblages indicate low energy conditions within

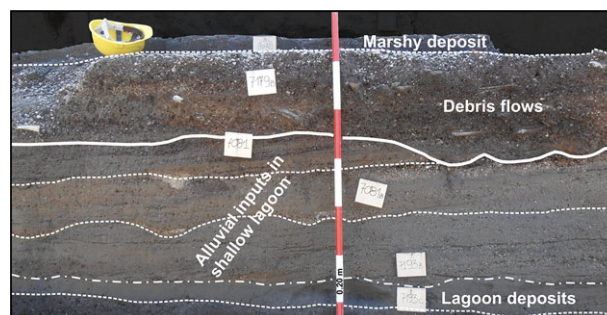


FIGURE 16 The final closure sequence of the harbor: the basal lagoon deposits (first half 5th century A.D.) are overlain by alluvial inputs in a shallow lagoon, showing multiple erosional surfaces. At the top, the arrival of debris flows (end of 5th to beginning of 6th century A.D.) in a subaerial environment is marked by a basal undulated, erosional contact. Spotty marsh deposits seal the sequence [Color figure can be viewed at wileyonlinelibrary.com]

an open lagoon, with a poorly vegetated bottom, as testified by the strong decrease in *Posidonia* remains.

The relative abundance of fine sand in the inner section (cluster G2) and the relative increase in the finer fraction in the outer one (cluster G3), which typifies the samples of this interval, is another evidence of the transition toward a more sheltered environment, characterized by depositional conditions favorable to decantation. At that moment, the lagoon occupied the whole area of Piazza Municipio.

The uppermost levels of the lagoon environment are only represented in log V2a and in the Top section. They are characterized by polygenic, heterometric, and poorly sorted sediments (cluster G4, Fig. 7A) gently inclined toward the open sea, by fragmented and reworked mollusk shells, and by the absence of ostracods (Fig. 11). The multiple erosional surfaces (Fig. 16) marking the deposition of these sediments are indicative of runoff and alluvial input into the shallow lagoon environment. The drastic increase in ARS (mean value 2 cm/yr, Fig. 12) recorded in this period testifies to the beginning of rapid infilling processes, causing the shoreline progradation and the consequent end of harbor activity in this bay sector, according to what was already recorded in Line 1. In fact, the water column at the beginning of the lagoon phase (top of lagoon sediments at 2.30 m b.s.l.) was reduced to ≈ 50 cm close to the quay. The latter was completely buried by sediments at the end of the 5th century A.D. Port activities migrated and continued farther eastward, as indicated by the archaeological remains unearthed in the Università excavation (Giampaola et al., 2006).

The topmost layers are represented by brownish, very poorly sorted sediments, devoid of mollusk remains, capped by a thin dark-grey silty-sand layer. The base of these units is characterized by an undulated erosional surface (Fig. 16). These characters suggest alluvial sedimentation in a subaerial environment, i.e., debris flow, which marks the final closure of the lagoon (Fig. 13). A large part of the Neapolitan-Vesuvian territory was affected in this period by debris flows, generated by the emplacement of ash deposits related to the A.D. 472 sub-Plinian Vesuvius eruption. This event resulted in a strong hydrogeological destabilization of an area larger than that directly affected by the emplacement of the pyroclastic deposits (Di Vito et al., 2016).

Subsequent ephemeral marshy episodes are testified by the spotty occurrence of thin dark silty layers at the top of the alluvial deposits (Figs 13 and 16).

6 | CONCLUSIONS

The Neapolis harbor excavations represent a unique opportunity to enrich our knowledge about the history of this important Roman town. The recovery of structures, such as piers, quays, thermal baths, and roads, has shed new light on the ancient town setting, coastal profile, and sea-level position from the 1st century B.C. up to the 6th century A.D. The archeological excavation together with the large amount of remains found in the harbor sediments provided a precise chronology of the infilling and allowed a detailed environmental history to be drawn on the basis of sedimentological and paleontological data.

The evolution of the harbor basin was determined by the interplay between natural and human-induced phenomena. In particular, the classic regressive trend which characterizes the natural evolution of a protected bay was enhanced by:

1. the dredging phases conducted until the 2nd century B.C., which engendered hypersedimentation due to the creation of a wide accommodation space;
2. the sedimentary input related to the A.D. 79 Pompeii eruption and the reworking of its sediments;
3. the construction of piers within harbor basin in the 1st century A.D., which induced restricted circulation and consequent hypersedimentation;
4. the increased alluvial input related to strong hydrogeological destabilization, connected to the A.D. 472 sub-Plinian Vesuvius eruption, which caused the final closure of the harbor bay.

The same causes, together with pollution induced since the 1st century A.D. by thermal bath effluent, contributed to environmental deterioration at the sea-bottom, engendering the drastic decrease in the *Posidonia* meadows.

Our investigation also identified primary deposits of the A.D. 79 Vesuvius eruption for the first time in the Neapolitan territory. These were attested through the recognition, both at the sea-bottom and on land, of an ash layer directly deposited by currents of the final, phreatomagmatic phases of the eruption.

Finally, the compositional data analysis approach proved valuable for interpreting the sedimentological and paleontological record of the ancient harbor of Neapolis. This valuable geoarchaeological tool can be applied to multiple paleoenvironmental proxy records in other cultural and geomorphic settings.

ACKNOWLEDGEMENTS

This article is dedicated to the memory of our friend and colleague Paola Romano. C. Morhange thanks IUF, Labex OT-Med (ANR-11-LABX-0061) and the A*MIDEX project (ANR-11-IDEX-0001-02). Daniela Mele of the University of Bari is acknowledged for the SEM

investigations on the ash samples. All figures, photographs and data included in this article have officially been authorized by the Soprintendenza Archeologia Belle Arti e Paesaggio of Naples. Two anonymous reviewers and the editors are thanked for their comments that greatly improved the original manuscript.

ORCID

Elda Russo Ermolli  <http://orcid.org/0000-0003-1275-6158>

REFERENCES

- AA.VV. (1985). *Napoli Antica*. Catalogo della mostra. Macchiaroli, Napoli.
- Aitchison, J. (1983). Principal component analysis of compositional data. *Biometrika*, 70, 57–65.
- Aitchison, J. (1986). *The statistical analysis of compositional data*. Monographs on statistics and applied probability (pp. 416). London: Chapman & Hall Ltd. (Reprinted in 2003 with additional material by The Blackburn Press)
- Aitchison, J., & Greenacre, M. (2002). Biplots of compositional data. *Applied Statistics*, 51(4), 375–392.
- Amato, L., Carsana, V., Cinque, A., Di Donato, V., Giampaola, D., Guastaferro, C., ... Russo Ermolli, E. (2009). Ricostruzioni morfologiche nel territorio di Napoli: L'evoluzione tardo pleistocenica-olocenica e le linee di riva in epoca storica. *Mediterranée*, 112, 23–31.
- Ayris, P. M., & Delmelle, P. (2012). The immediate environmental effects of tephra emission. *Bulletin of Volcanology*, 74, 1905–1936.
- Boetto, G. (2010). Le port vu de la mer: L'apport de l'archéologie navale à l'étude des ports antiques. In M., Dalla Riva (Ed.), *Meetings between cultures in the ancient mediterranean. Proceedings of the 17th International Congress of Classical Archaeology* (pp. 112–128). Rome: Ministero per i Beni e le Attività Culturali.
- Bony, G., Morhange, C., Bruneton, H., & Gébara, C. (2011). 2000 ans de colmatage du port antique de Fréjus (Forum Julii), France. Une double métamorphose littorale. *Comptes Rendues Geoscience*, 343, 701–715.
- Brancaccio, L., Cinque, A., Romano, P., Roskopf, C., Russo, F., Santangelo, N., & Santo, A. (1991). Geomorphology and neotectonic evolution of a sector of the Tyrrhenian flank of the southern Apennines (region of Naples, Italy). *Zeitschrift für Geomorphologie, Suppl. Bd*, 82, 47–58.
- Bruno, P. P. G., Rapolla, A., & Di Fiore, V. (2003). Structural setting of the Bay of Naples (Italy) seismic reflection data: Implications for Campanian volcanism. *Tectonophysics*, 72, 193–213.
- Caiazza, C., Ascione, A., & Cinque, A. (2006). Late Tertiary–Quaternary tectonics of the Southern Apennines (Italy): New evidences from the Tyrrhenian slope. *Tectonophysics*, 421, 23–51.
- Capasso, B. (1895). *Topografia della città di Napoli nell'XI secolo*. Napoli: A. Forni.
- Carey, S., & Sigurdsson, H. (1987). Temporal variations in column high and magma discharge rate during the AD 79 eruption of Vesuvius. *Geological Society American Bulletin*, 99, 303–314.
- Carsana, V., D'Amico, V., & Del Vecchio, F. (2007). Nuovi dati ceramologici per la storia economica di Napoli tra tarda antichità ed altomedioevo. In M., Bonifay, & J.C., Trèglia (Eds.), *Late Roman coarse wares, cooking wares and amphorae in the Mediterranean, archaeology and archaeometry* (pp. 423–437). Oxford: BAR International Series, 1662.
- Carsana, V., Febbraro, S., Giampaola, D., Guastaferro, C., Irollo, G., & Ruello, M.R. (2009). Evoluzione del paesaggio costiero tra *Parthenope* e *Neapolis*: Una sintesi geoarcheologica per l'area dell'antico porto. *Mediterranée*, 112, 15–22.

- Carsana, V., & Del Vecchio, F. (2010). Il porto di Neapolis in età tardo antica: Il contesto di IV secolo d.C. In S., Menchelli, S., Santoro, M., Pasquinucci, & G., Guiducci (Eds.), *Late Roman Coarse Wares, Cooking Wares and Amphorae in the Mediterranean, Archaeology and Archaeometry. Comparison between western and eastern Mediterranean* (pp. 459–470). Oxford: BAR International Series, 2185.
- Carsana, V., & Guiducci, G. (2013). I contesti ceramici di età medio imperiale dal porto di Neapolis. In L., Giron, M., Lazarich, & M., Conceicao Lopes (Eds.), *Actas del I Congreso Internacional sobre Estudios Ceramicos*. Cadice. (pp. 1007–1040), ISBN 978-84-9828-401-0.
- Cennamo, P., Caputo, P., Stefano, M., Russo Ermolli, E., & Barone Lumaga, M. R. (2014). Epiphytic diatom communities on sub-fossil leaves of *Posidonia oceanica* in the Graeco-Roman harbor of Neapolis: A tool to explore the past. *American Journal of Plant Science*, 5, 549–553.
- Cinque, A., Aucelli, P. P. C., Brancaccio, L., Mele, R., Milia, A., Robustelli, G., ... Sgambati, D. (1997). Volcanism, tectonics and recent geomorphological change in the bay of Napoli. *Supplementi Geografia Fisica e Dinamica Quaternaria*, 3(2), 123–141.
- Cinque, A., Irollo, G., Romano, P., Ruello, M. R., Amato, L., & Giampaola, D. (2011). Ground movements and sea level changes in urban areas: 5000 years of geological and archaeological record from Naples (Southern Italy). *Quaternary International*, 232(1), 45–55.
- Cioni, R., Bertagnini, A., Santacroce, R., & Andronico, D. (2008). Explosive activity and eruption scenarios at Somma-Vesuvius (Italy): A review. *Journal of Volcanology and Geothermal Research*, 178, 331–346.
- D'Agostino, B., & Giampaola, D. (2005). Osservazioni storiche e archeologiche sulla fondazione di Neapolis. In W. V., Harris & E., Lo Cascio (Eds.), *Noctes Campanae, Studi di storia antica e archeologia dell'Italia preromana e romana in memoria di Martin W. Frederiksen* (pp. 63–72). Napoli: Luciano Editore.
- Deino, A. L., Orsi, G., De Vita, S., & Piochi, M. (2004). The age of the Neapolitan Yellow Tuff caldera-forming eruption (Campi Flegrei caldera, Italy) assessed by $^{40}\text{Ar}/^{39}\text{Ar}$ dating method. *Journal of Volcanological and Geothermal Research*, 133, 157–170.
- Delile, H., Goiran, J.-P., Blichert-Toft, J., Arnaud-Godet, F., & Romano, P. (2016a). A geochemical and sedimentological perspective of the life cycle of Neapolis harbor (Naples, southern Italy). *Quaternary Science Reviews*, 150, 84–97.
- Delile, H., Keenan-Jones, D., Blichert-Toft, J., Goiran, J.-P., Arnaud-Godet, F., Romano, P., & Albarède, F. (2016b). A lead isotope perspective on urban development in ancient Naples. *PNAS*, 113, 6148–6153.
- Di Donato, V., Martin-Fernandez, J. A., Daunis-i-Estadella, J., & Esposito, P. (2015). Size fraction effects on planktonic foraminifera assemblages: A compositional contribution to the golden sieve rush. *Mathematical Geosciences*, 47(4), 455–470.
- Di Vito, M. A., Isaia, R., Orsi, G., Southon, J., de Vita, S., D'Antonio, M., ... Piochi, M. (1999). Volcanism and deformation since 12,000 years at the Campi Flegrei caldera (Italy). *Journal of Volcanological and Geothermal Research*, 91, 221–246.
- Di Vito, M. A., Zanella, E., Gurioli, L., Lanza, R., Sulpizio, R., Bishop, J., ... Laforgia, E. (2009). The Afragola settlement near Vesuvius, Italy: The destruction and abandonment of a Bronze Age village revealed by archaeology, volcanology and rock-magnetism. *Earth and Planetary Science Letters*, 277, 408–421.
- Di Vito, M. A., Castaldo, N., de Vita, S., Bishop, J., & Vecchio, G. (2013). Human colonization and volcanic activity in the eastern Campania Plain (Italy) between the Eneolithic and Late Roman periods. *Quaternary International*, 303, 132–141.
- Di Vito, M. A., de Vita, S., Rucco, I., Bini, M., Zanchetta, G., Boenzi, G., ... Stanco, E. (2016). Volcaniclastic debris flows related to 472 A.D. eruption at Vesuvius: Social and environmental impact from stratigraphic and geoarchaeological data. *Cities on Volcanoes*, 9, 20–25 November, Puerto Varas (Chile).
- Egozcue, J. J., Pawlowsky-Glahn, V., Mateu-Figueras, G., & Barceló-Vidal, C. (2003). Isometric logratio transformations for compositional data analysis. *Mathematical Geology*, 35(3), 279–300.
- Eynatten, H. V., Pawlowsky-Glahn, V., & Egozcue, J. J. (2002). Understanding perturbation on the simplex: A simple method to better visualise and interpret compositional data in ternary diagrams. *Mathematical Geology*, 34(3), 249–257.
- Folk, R. L. (1954). The distinction between grain size and mineral composition in sedimentary rock nomenclature. *Journal of Geology*, 62(4), 344–359.
- Giampaola, D., & Carsana, V. (2005). Neapolis Le nuove scoperte: La città, il porto e le macchine. In E., Lo Sardo (Ed.), *Eureka II degli antichi (Catalogo Mostra 2005)* (pp. 116–122). Napoli: Museo Archeologico Nazionale di Napoli.
- Giampaola, D., & Carsana, V. (2010). Fra Neapolis e Parthenope: Il paesaggio costiero ed il porto. In Blackman, D.J., & Lentini, M.C. (Eds.), *Ricoveri per navi militari nei porti del Mediterraneo antico e medievale* (pp. 119–129). Bari: Edipuglia.
- Giampaola, D., Carsana, V., Boetto, G., Crema, F., Florio, C., Panza, D., ... Pizzo, B. (2006). La scoperta del porto di Napoli: Dalla ricostruzione topografica allo scavo e al recupero dei relitti. *Marittima Mediterranea. International Journal of Underwater Archaeology*, 2, 47–91.
- Gurioli, L., Sulpizio, R., Cioni, R., Sbrana, A., Santacroce, R., Luperini, W., & Andronico, D. (2010). Pyroclastic flow hazard assessment at Somma-Vesuvius based on the geological record. *Bulletin of Volcanology*, 72, 1021–1038.
- Heiken, G. H. (1974). An atlas of volcanic ash. *Smithsonian Earth Science Contributions*, 12, 1–101.
- Heiken, G. H., & Wohletz, K. H. (1985). *Volcanic ash* (pp. 246). Berkeley: University of California Press.
- Kaniewski, D., Van Campo, E., Morhange, C., Guiot, J., Zviely, D., Shaked, I., ... Artzy, M. (2013). Early urban impact on Mediterranean coastal environments. *Nature Science Reports*, 3(3540), 1–5.
- Liuzza, V. (2014). Ricostruzione paleogeografica e paleoambientale della città di Napoli: Un'indagine geoarcheologica. Tesi di Dottorato in Scienze della Terra, XXVI ciclo. Università degli Studi di Napoli Federico II, 363 pp., Retrieved from <https://www.fedoa.unina.it>.
- Marriner, N., & Morhange, C. (2006). The 'ancient harbour parasequence': Anthropogenic forcing of the stratigraphic highstand record. *Sedimentary Geology*, 186, 13–17.
- Marriner, N., & Morhange, C. (2007). Geoscience of ancient Mediterranean harbours. *Earth Science Reviews*, 80, 137–194.
- Marriner, N., Morhange, C., Flaux, C., & Carayon, N. (2017). Harbors and ports. In A.S., Gilbert (Ed.), *Encyclopedia of geoarchaeology* (pp. 382–403). Berlin: Springer.
- Morhange, C., Blanc, F., Bourcier, M., Carbonel, P., Prone, A., Schmitt, S., ... Hesnard, A. (2003). Bio-sedimentology of the late Holocene deposits of the ancient harbor of Marseilles (Southern France, Mediterranean Sea). *The Holocene*, 13, 593–604.
- Morhange, C., Marriner, N., & Carayon, N. (2015). The geoarchaeology of ancient Mediterranean harbours. In G., Arnaud-Fassetta & N., Carcaud (Eds.), *French geoarchaeology in the 21st century* (pp. 281–289). Paris: CNRS editions, Alpha.
- Morhange, C., Marriner, N., & Carayon, N. (2016). Eco-history of ancient Mediterranean harbours. In T., Bekker-Nielsen, & R., Gertwagen (Eds.), *The inland seas, towards an ecohistory of the Mediterranean and the Black Sea* (pp. 85–106). Stuttgart: Franz Steiner, Verlag.
- Napoli, M. (1959). *Napoli greco-romana*. Napoli: Fausto Fiorentino Editore.

- Napoli, M. (1967). Topografia e archeologia. In: Storia di Napoli 1, 373–507. Napoli: Fausto Fiorentino Editore.
- Pawłowsky-Glahn, V., & Buccianti, A. (2011) (Eds.). *Compositional data analysis: Theory and applications* (400 pp.). New York: Wiley. ISBN: 978-0-470-71135-4.
- Peres, J.M. (1982). Major benthic assemblages, in: O. Kinne (ed.), *Marine Ecology, Ocean management. Part 1, ch. 8* (Vol. V, pp. 373–522). New York: John Wiley & Sons.
- Poveda, P. (2012). *Le navire antique comme instrument de commerce maritime: Restitutions 3D, tonnage, qualités nautiques et calculs hydrostatiques des épaves: Napoli A, Napoli C, Dramont E et Jules Verne 7* (PhD Thesis). Université Aix Marseille, Marseille.
- Quinn, G., & Keough, M. (2002). *Experimental Design and Data Analysis for Biologists* (pp. 557). Cambridge: Cambridge University Press.
- Romano, P., Di Vito, M. A., Giampaola, D., Cinque, A., Bartoli, C., Boenzi, G., ... Schiano di Cola, C. (2013). Intersection of exogenous, endogenous and anthropogenic factors in the Holocene landscape: A study of the Naples coastline during the last 6000 years. *Quaternary International*, 303, 107–119.
- Rossi, V., Sammartino, I., Amorosi, A., Sarti, G., De Luca, S., Lena, A., & Morhange, C. (2015). New insights into the palaeoenvironmental evolution of Magdala ancient harbour (Sea of Galilee, Israel) from ostracod assemblages, geochemistry and sedimentology. *Journal of Archaeological Science*, 54, 356–373.
- Ruello, M. R. (2008). *Geoarcheologia in aree costiere della Campania: I siti di Neapolis ed Elea -Velia. Tesi di Dottorato in Scienze della Terra, XX ciclo*. Università degli Studi di Napoli Federico II, Retrieved from <https://www.fedoa.unina.it>.
- Russo Ermolli, E., Romano, P., Ruello, M. R., & Barone Lamuga, M. R. (2014). The natural and cultural landscape of Naples (southern Italy) during the Graeco-Roman and the Late Antique periods. *Journal of Archaeological Science*, 42, 399–411.
- Sadori, L., Allevato, E., Bertacchi, A., Boetto, G., Di Pasquale, G., Giachi, G., ... Mariotti Lippi, M. (2015). Archaeobotany in Italian ancient Roman harbours. *Review of Palaeobotany and Palynology*, 218, 217–230.
- Seeliger, M., Bartz, M., Erkul, E., Feuser, S., Kelterbaum, D., Klein, C., ... Brückner, H. (2013). Taken from the sea, reclaimed by the sea - The fate of the closed harbour of Elaia, the maritime satellite city of Pergamum (Turkey). *Quaternary International*, 312, 70–83.
- Sgarrella, F., Di Donato, V., & Sprovieri, R. (2012). Benthic foraminiferal assemblage turnover during intensification of the Northern Hemisphere glaciation in the Piacenzian Punta Piccola section (Southern Italy). *Palaeogeography, Palaeoclimatology, Palaeoecology*, 333, 59–74.
- Sigurdsson, H., Cashdollar, S., & Sparkes, S. R. J. (1982). The eruption of vesuvius in A. D. 79: Reconstruction from historical and volcanological evidence. *American Journal of Archaeology*, 86(1), 39–51.
- Sigurdsson, H., Carey, S., Cornell, W., & Pescatore, T. (1985). The eruption of Vesuvius in A.D. 79. *Natural Geographic Research*, 1, 332–387.
- Stazio, A. (Ed.). (1988). Neapolis. Atti XXV Convegno di Studi sulla Magna Grecia, Taranto 3–8 ottobre 1985. Taranto: Istituto per la Storia e l'Archeologia della Magna Grecia.
- Wentworth, C. K. (1922). A scale of grade and class terms for clastic sediments. *Journal of Geology*, 30, 377–392.
- Zevi, F. (Ed.). (1995). Neapolis. Napoli: Edizioni Banco di Napoli.

SUPPORTING INFORMATION

Additional Supporting Information may be found online in the supporting information tab for this article.

How to cite this article: Di Donato V, Ruello MR, Liuzza V, et al. Development and decline of the ancient harbor of Neapolis. *Geoarchaeology*. 2018;1–16. <https://doi.org/10.1002/gea.21673>